JOURNAL OF AIRCRAFT
Vol. 30, No. 5, Sept.–Oct. 1993

Efficient Finite Element Method for Aircraft Deicing Problems

J. R. Huang,* Theo G. Keith Jr.,† and Kenneth J. De Witt‡
University of Toledo, Toledo, Ohio 43606

In this article a finite element formulation based on an assumed states method is proposed for the solution of heat conduction problems with phase change at a fixed temperature. Attention is directed towards reduction of computer cost through the use of an efficient formulation, solver, and algorithm. The procedure is applied to the analysis of an electrothermally deiced aircraft surface.

Nomenclature

C^* = apparent heat capacity
C_T = coefficient in Kirchhoff temperature function, dimensionless
c = specific heat capacity
H = enthalpy per unit volume
h = heat-transfer coefficient
k = thermal conductivity
L = latent heat of fusion for ice
$\boldsymbol{n}$ = unit normal vector
q = rate of heat generation per unit volume
T = temperature
T_∞ = ambient temperature
t = time
ΔT = a small temperature interval
θ = Kirchhoff variable
ρ = density

Subscripts
L = liquid
m = melting point or element node number
R = reference value
s = solid
w = two phase substance

Superscripts
n = time level
T = transpose
0 = initial condition

Introduction

THE numerical solution of phase-change problems has been a continuous research topic for many years. The principal difficulty in the modeling of a heat transfer problem with phase-change lies in the handling of the transformation between phases and the concomitant absorption (or liberation) of latent heat in the phase-change zone. The physics of the problem results in a temperature solution with a discontinuous temperature gradient at the phase transition interface. Also, the phase-change can take place either over a wide range of temperatures or at a single temperature.

A variety of numerical schemes have been proposed to overcome these difficulties. These schemes can be divided into essentially two categories: 1) methods with a moving interface, and 2) methods in which the interface is eliminated from consideration. In the first group, the energy equations for the solid region and the liquid region are solved simultaneously with an equation that gives the moving interfacial position. The latent heat of absorption (or liberation) is treated as a boundary condition. This method is capable of providing very accurate solutions. However, the major difficulty with this method is that the computational mesh must be redefined at each time step because of the movement of the phase transition zone. An alternate approach is to use methods which allow the mesh to adapt the moving phase front. However, these methods are complex and generally require considerable computer time.

A more general approach to phase-change problems is the so-called "enthalpy method" in which the phase change front is not simultaneously tracked during the computations, but located afterwards from calculated temperatures.[1–5] This approach is possible because the phase-front conditions are implicitly included in the enthalpy definition. The latent heat of absorption (or liberation) is accounted for by defining an apparent heat capacity. There are two possible formulations with this approach depending on whether temperature or enthalpy is chosen as the unknown variable. In the temperature formulation, it is necessary to carry out a smoothing of the enthalpy-temperature relation to define an apparent heat capacity. In the enthalpy formulation, there is implicit smoothing, which arises from the fact that the enthalpy varies continuously within the body being melted (or frozen), and across the moving front.

In order to prevent the reduction of lift on aircraft surfaces due to icing, various ice protection systems have been studied. Deicing methods are concerned with ice removal during and after ice buildup. An electrothermal deicer pad is a widely used thermal deicing system. In this method of aircraft wing surface ice control, heater pads are installed beneath the skin surrounding the leading edge of the wing, as shown in Fig. 1. The heaters are activated during icing conditions to remove any accreted ice. Electrical energy in the form of conducted heat destroys the adhesion forces at the ice/abrasion shield interface. Aerodynamic forces are then able to sweep the ice from the surface.

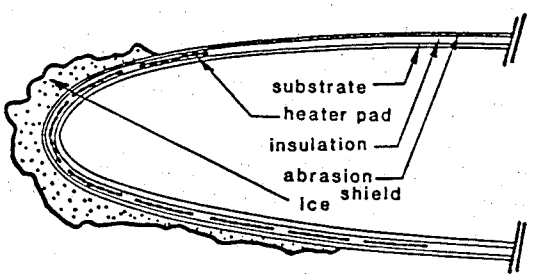

Fig. 1 Airfoil with electrothermal thermal deicer pad.

Presented as Paper 92-0532 at the AIAA 30th Aerospace Sciences Meeting and Exhibit, Reno, NV, Jan. 6–9, 1992; received Feb. 24, 1992; revision received July 7, 1992; accepted for publication July 10, 1992.

*Graduate Student, Mechanical Engineering Department. Student Member AIAA.
†Professor, Mechanical Engineering Department. Associate Fellow AIAA.
‡Professor, Chemical Engineering Department.

In any numerical simulation of an electrothermally deiced aircraft surface, it is necessary to deal with the phase-change problem and with the complexity of the airfoil geometry. In the past 20 yr most researchers have used finite difference methods to study deicer pads.[6,7] Recently, Huang et al.[8] applied an enthalpy method to simulate a two-dimensional electrothermally deiced aircraft surface with a finite element technique (FEM). It is well known that an FEM approach usually takes more CPU time than does a comparable finite difference approach. This disadvantage of FEM is apparent in a deicer pad simulation, since for a general two-dimensional problem the CPU time has been found to consume several hours on the VAX 6420. Hence, to extend this technique to a three-dimensional simulation of a deicer pad, it is necessary to improve the efficiency and reduce the computer costs. Possible approaches for reducing the computational time in a heat transfer problem with phase change that is solved by FEM include the following: 1) selection of an efficient computational method for treating the phase change problem; 2) selection of an efficient method for dealing with the stiffness matrix and the force vector, since the nonlinearities of phase-change problems cause most of the CPU time to be spent on the generation of these at each time step; 3) selection of an effective equation solver since the resulting set of algebraic equations is nonsymmetric; and 4) construction of an algorithm which is specially tailored to a parallel computing environment.

In 1984, Schneider and Raw[9] proposed a procedure (which has been called the "method of assumed states" by Roelke et al.[10] which significantly reduces the calculation cost and greatly improves the calculation speed in phase change energy transport problems. To date, this procedure has been used exclusively with finite difference methods.

The objectives of this article are 1) to present a numerical scheme in which the finite element method and the method of assumed states are used for the solution of aircraft deicing problems which include phase transformation, and 2) to develop an efficient solution strategy.

Analysis

Mathematical Model

The following assumptions were made in the development of a mathematical model for heat conduction with phase change.

1) The phase-change occurs at a single temperature rather than over a temperature range.

2) The physical properties are not strongly dependent on the temperature, i.e., constant values of heat capacity and conductivity will be applied in solid or liquid phase regions. For a specific temperature range, this assumption is quite reasonable. For example, the heat capacity and conductivity are, respectively, 0.5 Btu/lb$_m$-°F and 1.29 Btu/h-°F for ice at 32°F, whereas the heat capacity and conductivity are respectively 0.5 Btu/lb$_m$-°F and 1.54 Btu/h-°F at −40°F. The heat capacity and conductivity are, respectively, 1.0 Btu/lb$_m$-°F and 0.34 Btu/h-°F for water at 32°F, whereas, the heat capacity and conductivity are, respectively, 0.995 Btu/lb$_m$-°F and 0.4 Btu/h-°F at 200°F.

3) The density change due to melting is negligible, i.e., the effect of volume contraction during melting is neglected.

The general heat conduction equation is

$$(\rho c)\frac{\partial T}{\partial t} = \nabla\cdot(k\nabla T) + q \tag{1}$$

This expression can be used to determine the temperature distribution within any of the layers including that of the ice for an aircraft deicing simulation (Fig. 1). The heat source term, q, is zero everywhere except for the heaters.

The initial condition is

$$T = T^\circ \quad \text{at} \quad t = 0$$

The convective heat transfer boundary condition for either the bottom surface of the substrate or the ice layer-ambient interface (Fig. 1) is

$$k\nabla T\cdot \boldsymbol{n} = -h(T - T_\infty) \tag{2}$$

Enthalpy Formulation

The enthalpy method is used to determine the phase change within the ice. Equation (1) may be written in terms of the enthalpy per unit volume as

$$\frac{\partial H}{\partial t} = \nabla\cdot(k\nabla T) + q \tag{3}$$

where

$$dH = \rho c\, dT$$

or

$$H = \int_{T_R}^{T} (\rho c)_s\, dT \qquad T < T_m$$

$$H = \int_{T_R}^{T_m} (\rho c)_s\, dT + L + \int_{T_m}^{T} (\rho c)_L\, dT \qquad T \geq T_m \tag{4}$$

Note Eq. (3) can be applied in both the composite material and the ice for a deicer pad simulation since the composite material can be treated as a phase-change material which will always be in the solid state. Equation (3) may be written as

$$\frac{dH}{dT}\frac{\partial T}{\partial t} = \nabla\cdot(k\nabla T) + q$$

or

$$C^*\frac{\partial T}{\partial t} = \nabla\cdot(k\nabla T) + q \tag{5}$$

where C^* is the apparent heat capacity. There are numerous papers published that discuss how to determine the value of C^* when phase-change occurs over a temperature interval, e.g., Refs. 11–13. For this study, attention will be limited to a Stefan problem in which the phase-change occurs uniformly over a very small temperature range ΔT. Thus, we have

$$C^* = (\rho c)_s \qquad T < T_{m1}$$

$$C^* = (\rho c)_m + (L/\Delta T) \qquad T_{m1} < T < T_{m2}$$

$$C^* = (\rho c)_L \qquad T > T_{m2} \tag{6}$$

where the small temperature range $\Delta T = T_{m2} - T_{m1}$.

The total energy absorption (liberation) in the phase-change region can be divided into two parts: 1) sensible energy $(\rho c)_m\Delta T$, and 2) latent energy L. The temperature interval is taken to be so small that the sensible energy can be neglected for this problem. Thus, the apparent heat capacity in the mush region can be written as

$$C^* = \frac{dH}{dT} \approx \frac{\Delta H}{\Delta T} = \frac{(\rho c)_m\Delta T + L}{\Delta T} \approx \frac{L}{\Delta T} \tag{7}$$

Based on the discussion above, Eq. (4) can be simplified as

$$H = H_R + C^*T \tag{8}$$

where for the subcooled solid ($T \leq T_{m1}$)

$$H_R = 0$$

$$C^* = (\rho c)_s \tag{9}$$

for the two-phase region ($T_{m1} \leq T \leq T_{m2}$)

$$H_R = (\rho c)_s T_{m1} - (L/\Delta T) T_{m1}$$
$$C^* = (L/\Delta T) \tag{10}$$

and for the liquid phase ($T \geq T_{m2}$)

$$H_R = -(\rho c)_L T_{m2} + \rho_s c_s T_{m1} + L$$
$$C^* = (\rho c)_L \tag{11}$$

Equation (3) is nonlinear due to the dependence of thermal conductivity on temperature. This difficulty can be circumvented by applying the Kirchhoff transformation

$$\theta = \frac{1}{k_R} \int_{T_R}^{T(X,t)} k(T)\, dT \tag{12}$$

Using Leibnitz's formula gives

$$\nabla\theta = [k(T)/k_R]\nabla T$$

Equation (3) can be rewritten in a linear form as

$$\frac{\partial H}{\partial t} - k_R \nabla^2 \theta = q \tag{13}$$

The thermal conductivity of water may be taken to be piecewise continuous about the melt temperature. For a sufficiently small temperature interval about T_m (492°R), the following values may be used:

$$k = k_R = 1.416 \text{ Btu/h-ft-°F} \qquad T \leq T_{m1}$$
$$k = k_L = 0.320 \text{ Btu/h-ft-°F} \qquad T \geq T_{m2}$$

Combining the above values with Eq. (12), defining a reference temperature value, $T_R = 450$°R, and performing the integration, produces relationships between the temperature and the Kirchhoff variable in the solid, two-phase, and liquid regions:

$$\theta = T - T_R, \qquad T \leq T_{m1}$$
$$\theta = T - T_R, \qquad T_{m1} \leq T \leq T_{m2}$$
$$\theta = T_{m2} - T_R + (k_L/k_R)(T - T_{m2}), \qquad T \geq T_{m2} \tag{14}$$

Another advantage of using the Kirchhoff transformation for the finite element method is that when some of the nodes have a different phase than others of the same element, then the transformation helps avoid confusion as to physical properties of the element. Equation (14) can be simplified as

$$\theta = \theta_R + C_T T \tag{15}$$

where, for the subcooled solid ($T \leq T_{m1}$)

$$\theta_R = -T_R$$
$$C_T = 1 \tag{16}$$

for the two-phase region ($T_{m1} \leq T \leq T_{m2}$)

$$\theta_R = -T_R$$
$$C_T = 1 \tag{17}$$

and for the liquid phase ($T \geq T_{m2}$)

$$\theta_R = T_{m2} - T_R - (k_L/k_R) T_{m2}$$
$$C_T = (k_L/k_R) \tag{18}$$

Using coefficients H_R and C^* of Eq. (8) and coefficients θ_R and C_T of Eq. (15) produce expressions which are identical to those in Eqs. (4) and (14), respectively. In turn, this form reduces the set of equations to a single expression [Eq. (13)] to cover all three phases.

FEM Numerical Formulation

Equation (13) contains singularities due to the discontinuity in the temperature gradient and the enthalpy at the phase-change interface. To overcome this difficulty, a weak solution of Eq. (13) is sought. The solution may be defined as a pair of bound integrable functions H and θ, expressed in the following manner:

$$\int_\Omega \frac{\partial H}{\partial t} v\, d\Omega - \int_\Omega k\nabla\cdot(\nabla\theta) v\, d\Omega = \int_\Omega qv\, d\Omega \tag{19}$$

where v is an arbitrary test function and Ω is the volume. The importance of the weak solution is that certain numerical schemes will converge to the weak solution of the boundary value problem, despite discontinuities in the temperature gradient across the phase boundary. Consequently, it is not necessary to consider separate liquid and solid regions.

Equation (19) may be integrated by parts to obtain

$$\int_\Omega \frac{\partial H}{\partial t} v\, d\Omega + \int_\Omega k\nabla\theta\cdot\nabla v\, d\Omega - \int_{\partial\Omega} (k\nabla\theta)\boldsymbol{n} v\, dA = \int_\Omega qv\, d\Omega \tag{20}$$

where $\partial\Omega$ refers to the boundary of the volume Ω.

In the Galerkin method, the temperature within an element is approximated by a linear combination of basic functions

$$\theta(X, t) = [N][\theta]$$
$$H(X, t) = [N][H] \tag{21}$$

where $[N]$ is an interpolation vector

$$[N] = [N_1, N_2, \ldots, N_m]$$

The subscript m is the node number in an element. If v is replaced by the transpose of $[N]$, and Eq. (20) is utilized, then the following is produced[8]:

$$([K_3C^*]^{n+1} + [K_1C_T]^{n+1} + [K_2])[T]^{n+1} = [K_3C^*]^n[T]^n + [K_3H_R]^n - [K_3H_R]^{n+1} - [K_1][\theta_R]^{n+1} + [P_1]^{n+1} - [P_2]^{n+1} \tag{22}$$

where $[K_1]$, $[K_2]$, and $[K_3]$ are mass matrix, boundary condition matrix, and thermal inertia matrix, respectively, and $[P_1]$ and $[P_2]$ are heat source vector and boundary condition vector, respectively.

Equation Solution

The element expression, Eq. (22), can be assembled into a $m_1 \times m_1$ linear system of equations

$$[A][T]^{n+1} = [P] \tag{23}$$

where m_1 is the total node number of the system. In general, the resulting global matrix $[A]$ is nonsymmetric and must be updated at each time step.

One of the advantages for this formulation is it can be used to describe either the solid phase, the mushy region, or the liquid phase by simply assigning different phase coefficients H_R, C^*, θ_R, and C_T to the equations according to Eqs. (9–11) and (16–18). Once H_R, C^*, θ_R, and C_T are properly

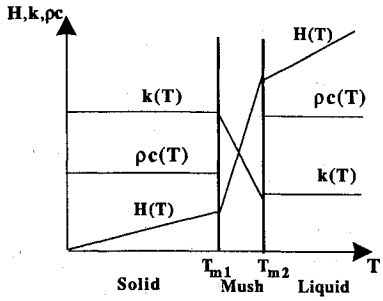

Fig. 2 Variation of heat capacity, enthalpy, and conductivity near the melting temperature.

defined, the entire system can be regarded as an ordinary heat conduction problem. What is more, phase-change is implicitly incorporated in the equation system. This makes equation solving for a deicer pad more efficient. Unfortunately, all of the discretization equations are nonlinear. The efficiency of the method is therefore limited by the efficiency of the technique employed to solve the discretization equations. The nonlinear aspects of the discretization equations are as follows:

1) Current H_R, C^*, θ_R, and C_T, or e.g., the current phase type, will depend on the current value of T, and it is not possible to formulate the numerical equations into a set of linear equations in the unknowns H_R, C^*, θ_R, and C_T.

2) Heat conductivity and heat capacity vary with temperature. Since attention is limited to materials whose physical properties are not strongly dependent on the temperature (Fig. 2), constant k and c will be used in both solid and liquid phases. In the mushy region C^* is used for all the time steps. Hence, the only nonlinear property that needs to be considered is k in the mushy region.

The assumed states method is used to overcome the first difficulty. The efficiency of this method makes it virtually a predictor-corrector scheme. All the nodal phases are assumed on the basis of the previous solution. After a new solution has been obtained, a correction is made to the phase distribution of the control volumes and a new solution is obtained again. This procedure is repeated until the phase distribution does not change between successive solutions. Furthermore, if the phase interface does not cross a control volume boundary during the time interval, a single iteration is all that is required. To prevent phase-change jumping, two rules have been given:

Rule 1: In any iteration, a node cannot transition directly from solid to liquid or from liquid to solid without passing through the intermediate two-phase region.

Rule 2: If the nodes which neighbor a node in the transition phase are both solid or liquid, then this node cannot be in the two-phase mushy region.

Schneider and Raw,[7] who introduced the method, stated that the procedure proved superior to conventional procedures with cost reductions ranging from a factor of 5 to 47. These observations tend to suggest that large cost reductions may be experienced for higher mesh refinement, larger time steps, or smaller values of the Stefan number.

The conductivity $k(T)$ in the mushy region is the only heat property which needs to be updated at each time step. This can be performed by an interpolation method based on the enthalpy at the same node

$$k_{\text{mush}} = k_L + (k_s - k_L)\frac{[H - (\rho c)_s T_m]}{[\rho_L c_s T_m + L - (\rho c)_s T_m]} \quad (24)$$

Accordingly, an algorithm may be suggested:

1) Assign H_R, C^*, θ_R, and C_T to each node based on its previous phase.

2) Calculate k_{mush} for the each node which is undergoing phase change.

3) Generate the element stiffness matrix and force vectors for each element.

4) Form a new $m_1 \times m_1$ global stiffness matrix by assembling each element matrix.

5) Solve the system of equations.

6) Check to determine whether the assumed phase at each node is correct, i.e., is the new phase based on the current temperature at each node the same as the previously assumed value? If yes, go to the next time step. Otherwise, reassign H_R, C^*, θ_R, and C_T to each node according to the new solution, and return to step 1.

Unfortunately, this algorithm is very expensive even for simulating a two-dimensional deicer pad whose node number is usually around 3500 and which has a bandwidth around 60. To extend this algorithm to a three-dimensional simulation would be impractical since most of the CPU time would be spent to reform a huge global matrix at each time step (steps 3 and 4) and to solve this system of equations (step 5). To improve the efficiency of this algorithm, steps 3–5 have to be reconsidered. In another words, a method of reforming the matrix and solving the developed system of equations must be sought in order to reduce the computation cost.

To begin this process, suppose that step 2 (the two-phase conductivity calculation) is skipped. From a careful review of Eq. (22), it may be seen that for this condition matrix $[A]$ will be invariant at time steps where no phase change occurs at any of the nodes. The boundary condition matrix $[K_2]$ is a constant during all the calculation time steps. The thermal inertia matrix term $[K_3][C^*]$ and the mass matrix term $[K_1][C_T]$ vary only when phase changes occur at some of the nodes. This indicates that most of the CPU time spent to reform the matrix is only because the conductivity of the two-phase region changes from k_s to k_L. However, it is not known how it changes, hence, an interpolation method is generally used to approximate this value. Also, as mentioned earlier, the essential mechanism to control the energy balance in the two-phase region is not the variation of the sensible energy, but the variation of the latent energy. To simulate this latent energy absorption (liberation), a very large apparent heat capacity has been assigned in this region. Therefore, it is not obvious what role the variation in the two-phase conductivity plays in such a complicated situation. From the considerations above, a new algorithm based on a constant conductivity k_R applied to two-phase regions is proposed.

The benefit of new algorithm not only stems from the cost saving of reforming and reassembling a matrix at the time step without phase changes at nodes, but also in the cost saving of solving the system of equations by way of a properly chosen solver. The solution of the algebraic systems of equations consumes a considerable amount of computing time. The performance of the algorithm depends critically on the choice of the solver. The most widely used solvers in FEM applications are Cholesky's method and the conjugate gradient method. These have been mainly applied to symmetric matrix problems.[14]

For this study, a direct method, the LU decomposition method, was chosen. This selection was made because the matrix is nonsymmetric and for several other reasons which will become clear from the following.

Matrix $[A]$ in Eq. (23) is a nonsingular $m_1 \times m_1$ matrix. Replacing $[A]$ with LU, where L is a lower triangular matrix and U is an upper triangular matrix, and factoring gives

$$[A][T] = LU[T] = L(U[T]) = [P] \quad (25)$$

Let $[Z] = U[T]$

The solution is then found using forward and backward substitution

$$L[Z] = [P]$$
$$U[T] = [Z] \quad (26)$$

It is well known that the decomposition of LU is not affected by the change of the right side of Eq. (23). Since matrix $[A]$ will be invariant if no phase-change occurs at any nodes, there is the potential to save the cost of the LU decomposition of the matrix $[A]$ during the operations of nonphase change time steps. If all the nodes retain their phase at M successive time steps, the total number of arithmetic using LU decomposition to solve Eq. (23) until next phase change occurs is $m_1^3/3 + Mm_1^2$. By using the Gaussian elimination algorithm, $Mm_1^3/3 + Mm_1^2$ operations will be required (a considerable increase for any $M > 1$). Therefore, in the event that no phase-change occurs at any node of the system, the solution of the linear system Eq. (23) can be directly obtained by just repeating forward and backward substitution. Most importantly, all costs of reforming, reassembling of matrix $[A]$ and LU decomposition of matrix $[A]$ are saved.

There are several other techniques which can be used to further reduce the computational time of this method:

1) Since boundary matrix $[K_2]$ and vector $[P_2]$ are invariant during the entire calculation, they can be put into matrix $[A]$ and vector $[P]$ need not be updated.

2) For the deiced airfoil simulation, the ice is initially in a solid phase (melting problem), therefore, the coefficient matrix will be symmetric prior to phase-change. The amount of calculation may be further reduced by factoring matrix $[A]$ into LL^T by Cholesky's method.

A revised or new algorithm can now be written as follows:

1) Form symmetric matrix $[A]$ using Eq. (23).
2) Factor matrix $[A]$ into LL^T by Cholesky's method.
3) Form vector $[P]$ using Eq. (23).
4) Use backward and forward substitution to solve for $[T]^{n+1}$.
5) Check if phase-change occurs at any node; if not, go to step 3, otherwise continue.
6) Form and assemble the nonsymmetric matrix $[A]$.
7) Perform LU decomposition by Crout's method.
8) Form vector $[P]$ using Eq. (23).
9) Solve $[T]^{n+1}$ by backward and forward substitution.
10) Check if phase-change occurs at any node, if not, go to step 8 to calculate the solution for next time step. Otherwise go to step 6.

Finally, it should be noted that another advantage in using LU decomposition is that round-off error can be greatly reduced by using double-precision to handle the summation (inner products). For an aircraft deicing simulation this is especially important since the extremely small layer thicknesses as compared to the airfoil chord length make round-off error considerations very important. For example, when the node number exceeds 600, Gaussian elimination usually becomes unstable. But by using LU decomposition, the results maintain high accuracy, even for a very large system of equations.

Table 1 provides an indication of the magnitude of time saving obtained by utilization of this algorithm: (all examples were run on a VAX 6420).

Table 1 Comparison of CPU times for two algorithms

Band width	Element number	Node number	Time steps	CPU times, s Old algorithm	CPU times, s New algorithm
30	1,550	1,000	200	1,150	210
65	3,800	2,800	200	10,000	1,400

Table 2 Comparison of CPU times between sequential computer and supercomputer

	CPU times, s Old algorithm	CPU times, s New algorithm
Sequential algorithm (VAX 6420)	1325	220
Vectorized algorithm (Cray X-MP)	68	11.15

Vectorization and Parallelization

It is well known that the key to achieving optimum performance on supercomputers is through the modification of an existing algorithm or by the development of a method tailored to a parallel computing environment.[15,16] The following example gives only a rough idea what the difference is between sequential and vectorized algorithms. For a problem node number totaling 1250, an element number equal to 2500, and a band width of 38, CPU times are listed in Table 2 for both the new and the old algorithms, for both the VAX (sequential algorithm) and the Cray X-MP (vectorized algorithm) machines.

Results and Discussion

Comparisons with Analytical Results

Two test problems are considered here to compare the numerical predictions to analytical solutions. In both problems, the conductivities of the solid phase and liquid phase are identical. Hence, there are no differences between the old and new algorithms. Both problems were analyzed previously by Rolph and Bathe.[17] The purposes for these comparisons are to verify that the basic formula, Eq. (21), is correct for both one- and two-dimensional problems.

1) Consider a one-dimensional freezing problem in a semi-finite half-space with fixed temperature $T < 0$ at the surface $x = 0$ (Fig. 3). The thermal properties are $(\rho c)_s = (\rho c)_L = 1.0$ Btu/in.^{3}-°F, $k_s = k_L = 1.0$ Btu/in.-sec-°F and $L = 0.25$ Btu/in.^{3}

Comparisons of the predicted front position and temperature history for the length of the first 4 in. with the analytical solution are shown in Figs. 4 and 5. As can be seen, good agreement has been obtained.

2) Consider the corner of a uniform infinite container of a liquid with an initial temperature 0.3°F and a freezing temperature 0.0°F (see Fig. 6). At time $t = 0$, the temperature of surfaces, $T(x, 0)$ and $T(0, y)$, are reduced to 1-deg below the freezing temperature and are maintained constant. Other test conditions are same as the first problem. Comparisons of the front position and temperature history of point A ($x = 0.5$ and $y = 0.5$) with the analytical solution are shown in Figs. 7 and 8.

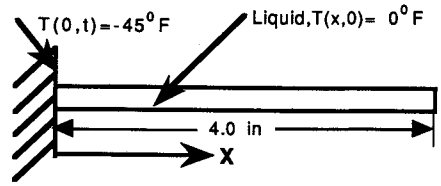

Fig. 3 One-dimensional test problem.

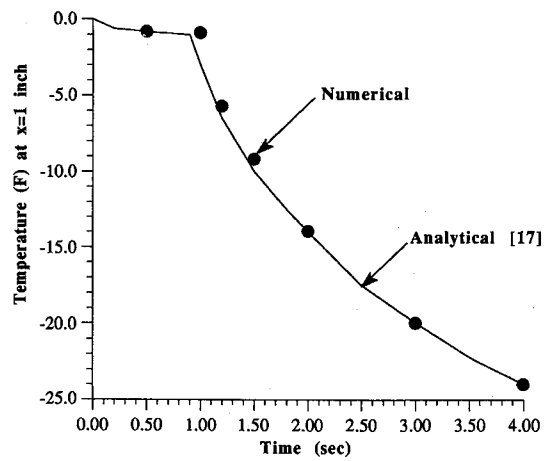

Fig. 4 Comparison of predicted temperatures with analytical data.

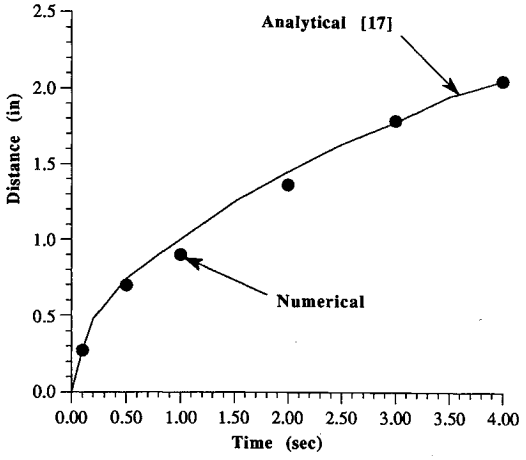

Fig. 5 Comparison of predicted front position with analytical data.

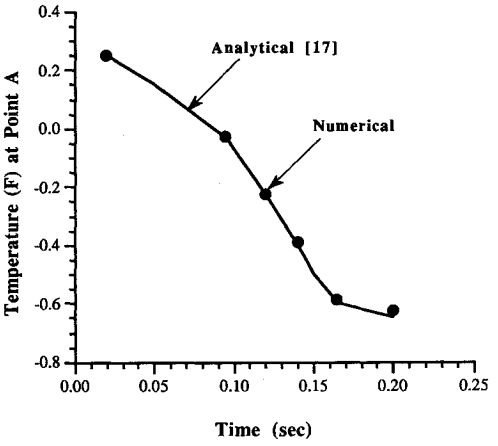

Fig. 7 Comparison of predicted temperature with analytical data.

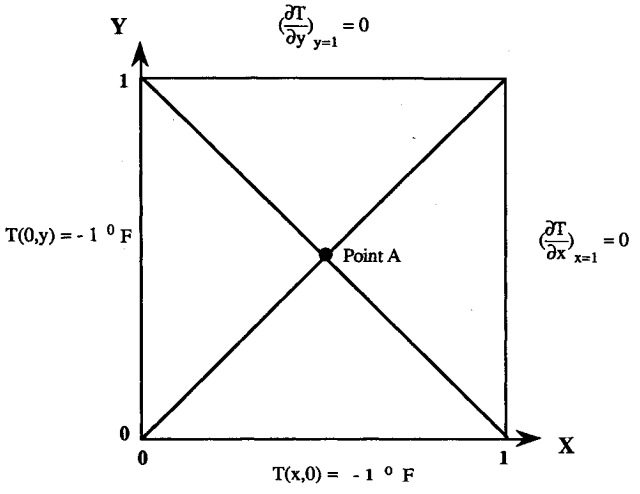

Fig. 6 Two-dimensional test problem.

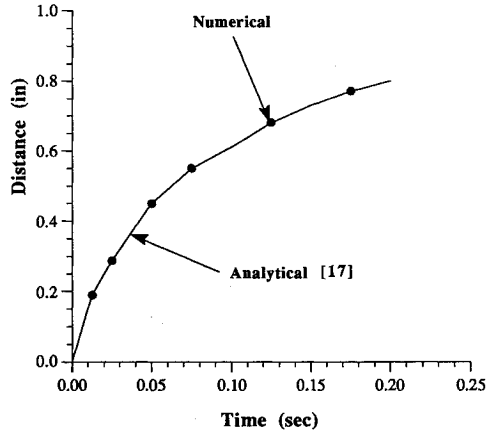

Fig. 8 Comparison of predicted front position with analytical data.

Table 3 Deicer pad property values

Layer name	Material	Thickness, in.	Conductivity, Btu/ft-h-°F	Specific heat, Btu/lb_m-°F	Density lb_m/ft^3
Substrate	75s-T6 Aluminum	0.087	66.5	0.26	155
Inner insulation	Epoxy/glass	0.05	0.22	0.23	110
Heater	Nichrome	0.004	7.6	1.00	55.07
Outer insulation	Epoxy/glass	0.01	0.22	0.23	110
Shield	304 Stainless steel	0.012	8.7	0.117	495
Ice	Ice or water	0.25	1.29 or 0.32	0.5 or 0.99	57 or 62

Comparisons Between Two Algorithms

One- and two-dimensional simulations of a standard deicer pad whose composite structure is simplified to five layers have been used here for comparing the results of the new and old algorithms. The properties of the materials are listed in Table 3. For both simulations, the heater power is 30 W/in.^{2}, the ambient and initial temperatures are 10°F, the inner convection coefficient is 10 Btu/h-ft^2-°F, and the outer convection coefficient is 150 Btu/h-ft^2-°F.

One-Dimensional Simulation

A slice of the composite airfoil structure was used for the one-dimensional analysis. This problem has been solved using 64 elements. Node 28 is at the ice/abrasion shield interface, 29 is the first node within the ice, etc. Figure 9 is the temperature histories of node 28 solved by the two different algorithms. Apparently, from a time of 4.5–11 s, the results obtained by the new algorithm are higher than those of the old algorithm. But this difference is gradually reduced afterwards. Figure 10 plots the same temperature history for a time interval of 60 s to demonstrate that the difference between the two algorithms disappears at longer times. To further understand these differences, Fig. 11 is a plot of the temperature history of nodes 29–31 for a time interval of 60 s obtained by using both the old and new algorithms. Based on these comparisons, the following major points can be summarized:

1) The temperature histories obtained by the new algorithm or old algorithm are very close for the nodes which are in solid phases or two phases.

2) After a node completes the phase-change and enters the liquid phase, then if its neighboring node undergoes a phase-change during this period, the temperature obtained by the new algorithm is higher than the temperature obtained by the old algorithm.

3) After the neighboring next node completes its phase-change, the solution differences between the two algorithms gradually disappear.

The difference between the results from the two algorithms is due to the fact that different methods are used to assign k to the nodes which are undergoing phase change; in the old algorithm, an interpolation method is used to calculate k at

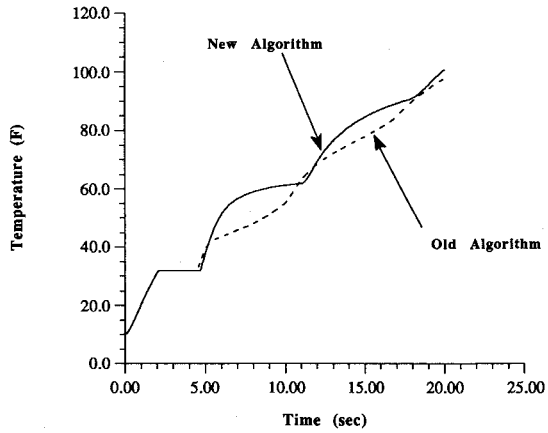

Fig. 9 Temperature history of ice/abrasion shield interface node (over 20 s).

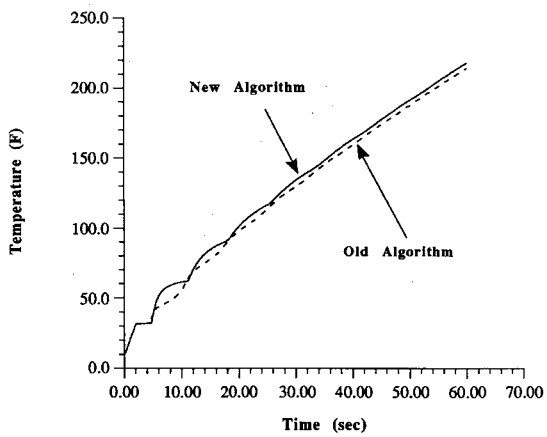

Fig. 10 Temperature history of ice/abrasion shield interface node (over 60 s).

each time step; in the new algorithm a constant k is applied. For further understanding how different k values can give different effects, assume that the $i - 1$ node is the liquid phase, node i is undergoing a phase change and node $i + 1$ is in the solid phase (Fig. 12). In the old algorithm

$$k_{e-1} = (k_{i+1} + k_i)/2 = (k_L + k_m)/2$$
$$k_e = (k_i + k_{i+1})/2 = (k_m + k_s)/2 \qquad (27)$$

where the two-phase conductivity k_m is changed at each time step. But in the new algorithm

$$k_{e-1} = k_L$$
$$k_e = k_s \qquad (28)$$

The heat fluxes q_{i-1}, q_i, and q_{i+1} to and from the adjacent elements are related to average temperatures in the elements, i.e.

$$q_{i-1} = k_{i-1}[(T^{\text{ave}}_{e-2} - T^{\text{ave}}_{e-1})/\Delta x]$$
$$q_i = k_i[(T^{\text{ave}}_{e-1} - T^{\text{ave}}_{e})/\Delta x]$$
$$q_{i+1} = k_{i+1}[(T^{\text{ave}}_{e} - T^{\text{ave}}_{e+1})/\Delta x] \qquad (29)$$

When all the nodes are in the solid phase, the conductivities will take the value of k_s for both algorithms, hence, the simulation results are the same. However, when node i starts to change phase, the apparent heat capacity of node i has been assigned a very large value. As a result, this node behaves like a sink of energy which consumes almost all of the energy q_{i-1} coming from element $e - 1$. As a result of the fact all the q_{i-1} has been absorbed by the node i, there is only a very small amount of energy left which will be transferred to the next element as q_i and all the temperatures of the nodes beyond node i, therefore, will not show much variation. This fact makes the exact determination of the conductivity in element e not of vital importance since heat transport beyond e is almost zero. As an informal confirmation of this analysis, it is interesting to point out that the simulation results remain almost the same if values ranging from 1.0 to 10.0 are assigned to k_e and the same problem is rerun. Therefore, it is not surprising that the simulation results are very close between the two algorithms for nodes $i + 1$, $i + 2$, . . . , etc., since the difference of the conductivities is far smaller than the maximum difference over this range.

The difference of k_{e-1} between the two algorithms does substantially change the simulation results. The temperature of node $i - 1$ of the new algorithm shows a slightly higher result than obtained by the old algorithm. This can be understood by reviewing Eqs. (27) and (28). The old algorithm uses a larger k_{e-1} value than the new algorithm since k_m is always larger than k_L. From Eq. (29), it can be seen that the value of q_{i-1} of the old algorithm is therefore larger than the q_{i-1} of new algorithm. This means that more energy will transfer to the neighboring elements for the old algorithm, and as the result, the temperature of node $i - 1$ is lower than the value obtained by the new algorithm. Obviously, this will force node i to complete its change of phase earlier than predicted by

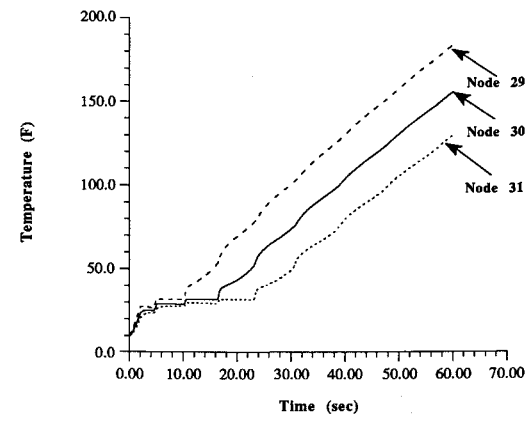

a) Old algorithm

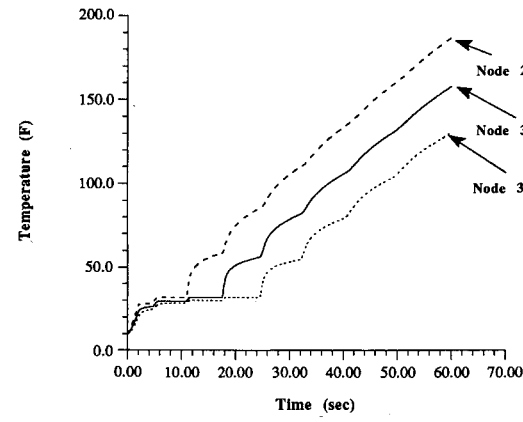

b) New algorithm

Fig. 11 Temperature history of first three nodes above abrasion shield interface.

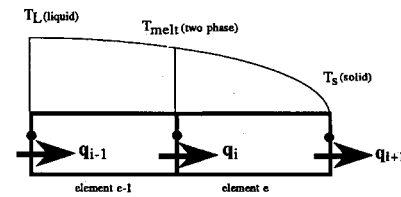

Fig. 12 Elements, nodes, and heat flux.

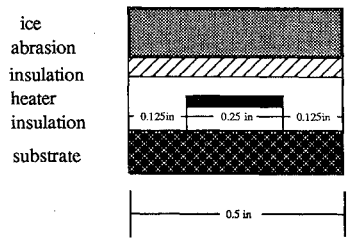

Fig. 13 Two-dimensional deicer model.

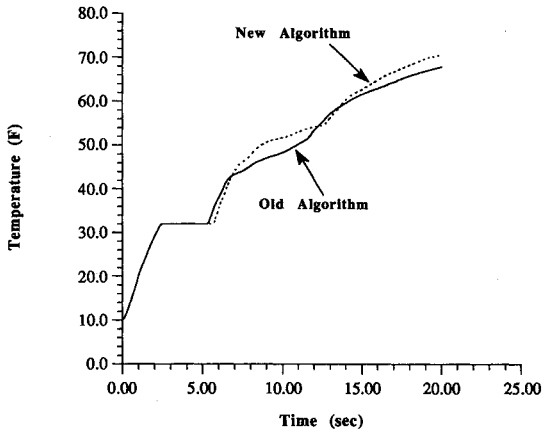

Fig. 14 Temperature history of ice/abrasion shield interface node (20 s).

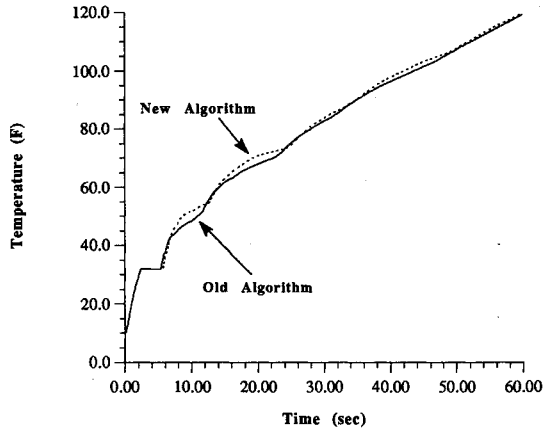

Fig. 15 Temperature history of ice/abrasion shield interface node (60 s).

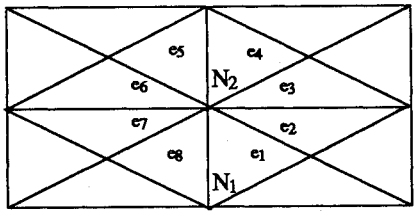

Fig. 16 Nodes and elements of a two-dimensional model.

the new algorithm, since node i accepts more energy (q_{i-1} is larger). The reasons which did not apparently change the solution of the phase change are as follows:

1) The difference of the q_{i-1} between the two algorithms is quite small compared to the latent heat value which node i needs to consume in order to complete its phase change.

2) Secondly, and the more important reason, the melting time lag between the two algorithms does not accumulate as the phase-change front passes to the next node. As node i completes its phase-change, the value of k_{e-1} will be k_L for both algorithms. Then node $i-1$ of the old algorithm will require more energy to satisfy the balance of energy of the governing equation. During this period, it provides less energy q_{i-1} to node i. In other words, the difference between the two algorithms is only that node i first gets more energy before it completes the phase change, then it gets less energy after it completes phase-change for the old algorithm. Comparison of the simulation results between the two algorithms has confirmed this analysis. All temperature differences between the two algorithms has disappeared after its nearest neighboring node completes the phase-change, and therefore, the phase-change time does not show an increase for the new algorithm as the phase-changes goes on.

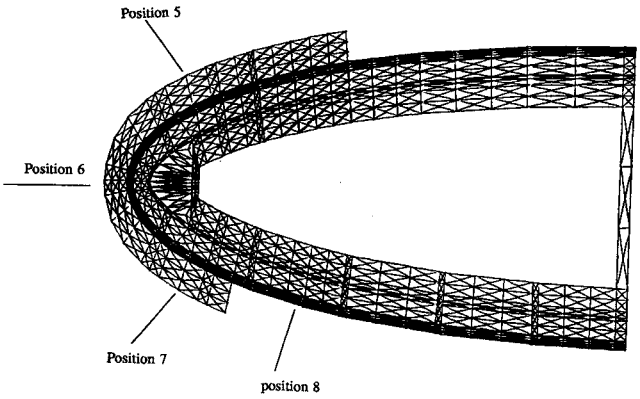

Fig. 17 FEM mesh for an airfoil consisting of 14 layers.

Table 4 Data for experimental deicer pad

Layer	Thermal thickness, in.	Thermal conductivity, Btu/h-ft-°F	Diffusivity, ft²/h
Stainless steel abrasion shield	0.0300	8.70	0.1500
Epoxy adhesive	0.0168	0.10	0.0058
Epoxy/glass insulation	0.0138	0.22	0.0087
Epoxy adhesive	0.0082	0.10	0.0058
Copper heater element	0.0065	60.00	1.1500
Epoxy adhesive	0.0082	0.10	0.0058
Epoxy/glass insulation	0.1338	0.22	0.0087
Epoxy adhesive	0.0082	0.10	0.0058
Stainless steel blade skin	0.0200	8.70	0.1500
Epoxy adhesive	0.0100	0.10	0.0058
Aluminum doubler	0.0500	102.00	2.8300
Epoxy adhesive	0.0100	0.10	0.0058
Aluminum substrate	0.1750	102.00	2.8300

Table 5 Test conditions for a two-dimensional simulation

Blade position	Ice thickness, in.	Heater power, W/in.²	Heater on/off times, s
3	0.0	0.0	
4	0.0625	15.7	165/175, 225/235, 285/295
5	0.0625	15.8	165/175, 225/235, 285/295
6	0.0	15.9	165/175, 225/235, 285/295
7	0.0625	16.0	155/165, 215/225, 275/285
8	0.0	16.3	175/185, 235/245, 295/305

Deicing test commences after ice has accreted for 155 s.
Ambient temperature = 20°F.
Outer convection coefficient = 70 Btu/h-ft²-°F.
Inner convection coefficient = 10 Btu/h-ft²-°F.
Each heater element is 1-in. wide.
Gap between heaters is 0.061 in.

Two-Dimensional Simulation

A section of the composite structure of the deicer used for the two-dimensional analysis is shown in Fig. 13. All the test

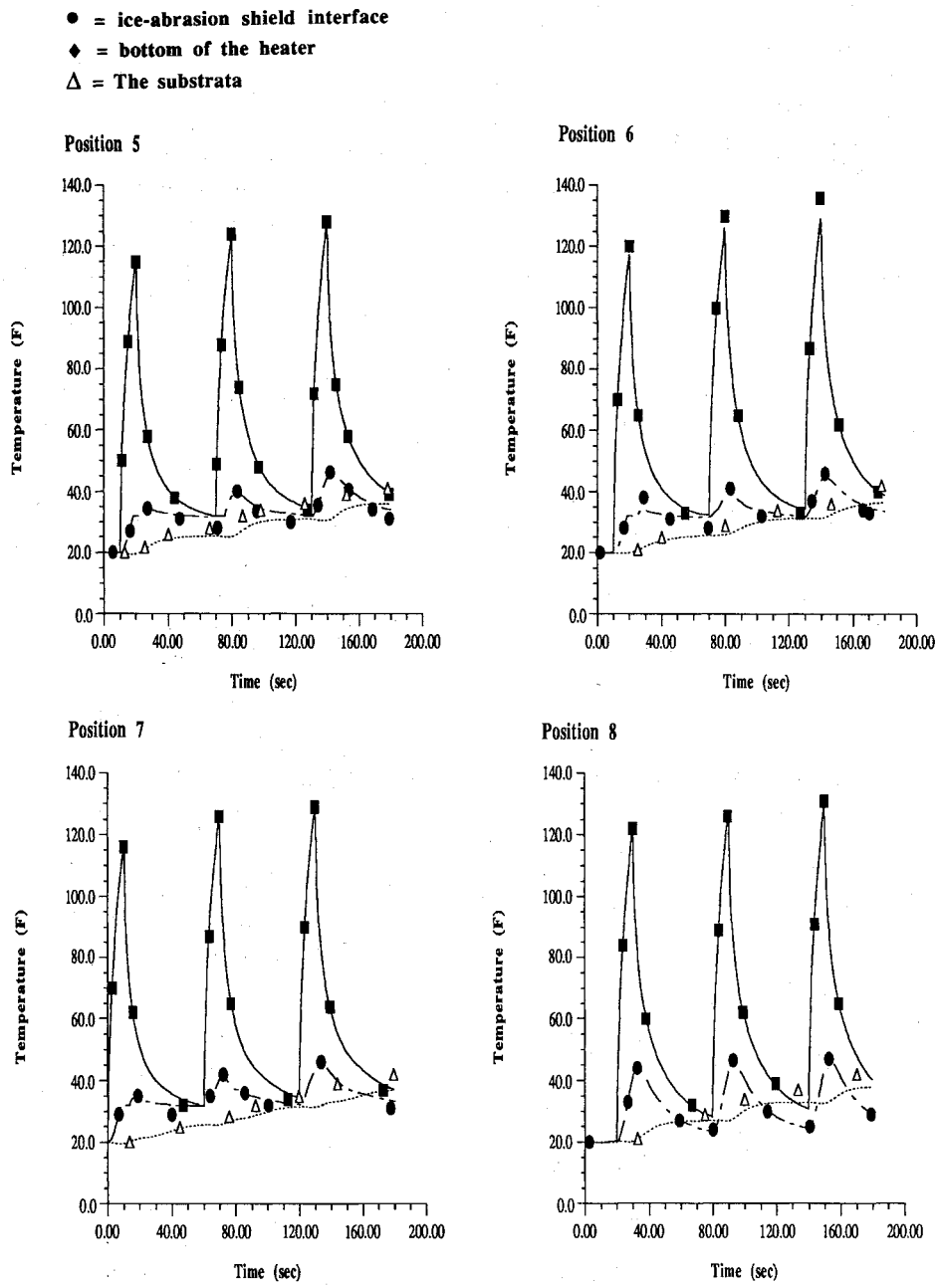

Fig. 18 Comparison of predicted temperature (solid line) with experimental data (symbols).

conditions are same as those for the one-dimensional problems except there are gaps at the two sides of the heater. The temperature variations of the shield/ice interface with time obtained by the two algorithms are shown in Fig. 14. Figure 15 are plots of the temperature history at the shield/ice interface over a 60-s interval to make certain agreement is obtained between the algorithms. The data shown in Fig. 15 reveals the difference between the two algorithms becomes smaller than the difference for the one-dimensional case. This can be explained by the use of Fig. 16. If node N_1 is undergoing phase-change, it has a different conductivity than the surrounding nodes. The conductivity of each element is the average value of its vertex nodes. Elements e_1 and e_8 have smaller conductivities compared to the other elements since they have N_1 as one of their vertices. Now consider node N_2, one of node N_1 neighbors. The conductivity of node N_2 will be affected by the node N_1 through elements e_1 and e_8. But this effect becomes very weak after assembling since the node N_2 is the common vertex of elements e_2, e_3–e_7. Each element contributes to the effect on node N_2. The effects of elements e_1 and e_8 are hardly seen among them. Hence, it is to be expected that the difference between the two algorithms becomes even smaller in three-dimensional simulations since one node will be shared as a common vertex by even more elements.

Comparison with Experimental Data

Predictions for a two-dimensional simulation of the electrothermal deicing of aircraft components using the new algorithm were compared to existing experimental data.[18] The essential purpose for this comparison is to demonstrate that the new algorithm adequately handles a real case. The mesh representation of a deicer pad is illustrated in Fig. 17. The pad consists of 14 layers which includes an ice layer (Table 4). Six heaters are modeled, all of which are fired separately and have slightly different power densities. Test conditions are listed in Table 5. When ice is present on the blade, it is modeled as having a constant value of 0.0625 in. As can be seen from Fig. 18, at position 8, excellent agreement with the experiment data has been obtained. This is not surprising since there is no ice present at position 8. At positions 5 and 7, the predictions agree reasonably with the experimental data. The

numerical simulation results at position 6 (stagnation point) are a little lower than the experimental result.

Conclusions

A temperature-based finite element formulation and algorithm have been developed for the solution of a nonlinear equation resulting from a phase-change problem. This formulation and algorithm have been found to be superior to conventional FEM procedures with cost reductions ranging from 5 to 50 times. The degree of the computer time reduction of the new algorithm strongly depends on the total node number of the phase-change in the calculation, and the node number whose phase-change occurs at the same time.

A modified algorithm which exploits both vectorization and parallelization on a supercomputer to minimize computational effort is utilized. The computational time reduction is usually related to the length of the processed array. For a typical electrothermal deicer pad problem, the reduction is around 20 times for both new and old algorithms.

The finite element formulation and algorithm associated with the phase-change problem presented here greatly reduces the CPU time. This enables the algorithm to be used as a powerful design tool in applications related to the phase-change problems such as an aircraft deicing pad. This offers the potential to further extend the simulation to a three-dimensional geometry and to more complex applications.

Acknowledgment

The authors wish to thank the NASA Lewis Research Center for their continuous financial support of this work.

References

[1]Dalhuijsen, A. J., "Comparison of Finite Element Techniques for Solidification Problems," *International Journal for Numerical Methods in Engineering*, Vol. 23, 1986, pp. 1807–1829.

[2]Donald, R. W., III, and Bathe, K. J., "An Efficient Algorithm for Analysis of Nonlinear Heat Transfer with Phase Changes," *International Journal for Numerical Methods in Engineering*, Vol. 18, 1982, pp. 119–134.

[3]Voller, V. R., and Cross, M., "Accurate Solutions of Moving Boundary Using the Enthalpy Method," *International Journal of Heat and Mass Transfer*, Vol. 24, 1981, pp. 545–556.

[4]Tacke, K. H., "Discretization of the Explicit Enthalpy Method for Planar Phase Change," *International Journal for Numerical Methods in Engineering*, Vol. 21, 1985, pp. 543–554.

[5]Crivelli, L. A., and Idelsohn, S. R., "A Temperature-Based Finite Element Solution for Phase Change Problems," *International Journal for Numerical Methods in Engineering*, Vol. 21, 1986, pp. 99–119.

[6]Wright, W. B., Keith, T. G., Jr., and De Witt, K. J., "Transient Two-Dimensional Heat Transfer Through a Composite Body with Application to Deicing of Aircraft Components," AIAA Paper 88-0358, Jan. 1988.

[7]Keith, T. G., Jr., De Witt, K. J., Wright, W. B., and Masiulaniec, K. C., "Overview of Numerical Codes Developed for Predicted Electrothermal De-Icing of Aircraft Blades," AIAA Paper 88-0288, Jan. 1988.

[8]Huang, J. R., Keith, T. G., Jr., and De Witt, K. J., "Numerical Simulation of an Electrothermal De-Iced Aircraft Surface Using the Finite Element Method," AIAA Paper 91-0268, Jan. 1991.

[9]Schneider, G. E., and Raw, M. J., "An Implicit Solution Procedure for Finite Difference Modeling of the Stefan Problem," *AIAA Journal*, Vol. 22, Nov. 1984, pp. 1685–1690.

[10]Roelke, R. J., Keith, T. G., Jr., De Witt, K. J., and Wright, W. B., "Efficient Numerical Simulation of a One-Dimensional Electrothermal Deicer Pad," *Journal of Aircraft*, Vol. 25, No. 12, 1988, pp. 1097–1105.

[11]Mogan, K., Lewis, R. W., and Zienkiewicz, O. C., "An Improved Algorithm for Heat Conduction Problem with Phase Change," *International Journal for Numerical Methods in Engineering*, Vol. 12, 1978, pp. 1191–1195.

[12]Giudice, D., Comini, G., and Lewis, R. W., "Finite Element Simulation of Freezing Processes in Soils," *International Journal in Numerical Methods in Geomechanics*, Vol. 2, 1978, pp. 223–235.

[13]Lemmon, E. C., "Phase Change Techniques for Finite Element Conduction Codes," *Numerical Methods in Thermal Problems, Proceedings of the First International Conference*, Pineridge Press International, Swansea, Wales, UK, July 1979, pp. 149–158.

[14]Kobayashi, T., and Haito, H., "Large-Scale Finite Element Analysis with Supercomputers," *Journal of Information Processing*, Vol. 11, No. 1, 1987, pp. 47–52.

[15]VanLuchene, R. D., Lee, R. H., and Meyers, V. J., "Large Scale Finite Element Analysis on a Vector Processor," *Computer and Structures*, Vol. 24, No. 4, 1986, pp. 625–635.

[16]Geohlich, D., Komzsik, L., and Fulton, R. E., "Application of a Parallel Equation Solver to Static FEM Problems," *Computer and Structures*, Vol. 31, No. 2, 1989, pp. 121–129.

[17]Rolph, W. D., III, and Bathe, K., "An Efficient Algorithm for Analysis of Nonlinear Heat Transfer with Phase Changes," *International Journal for Numerical Methods in Engineering*, Vol. 18, 1982, pp. 119–134.

[18]Leffel, K. L., "A Numerical and Experimental Investigation of Electrothermal Aircraft Deicing," M.S. Thesis, Univ. of Toledo, Toledo, OH, Jan. 1986.